

Permanent oscillations and solitary wave behavior in flatband Heisenberg quantum spin systems

Jannis Eckseler^{1,*} and Jürgen Schnack^{1,†}

¹*Fakultät für Physik, Universität Bielefeld, Postfach 100131, D-33501 Bielefeld, Germany*

(Dated: February 6, 2025)

Research on the emergence of thermodynamics in closed quantum systems under unitary time evolution arrived at the consensus that generic systems equilibrate under rather general assumptions. A new focus of the field is thus on exceptions. Persistent oscillations are one possible hallmark of non-ergodic time evolution. While time-crystalline behavior results from, e.g., many-body localization, here we show that ever-revolving solitary waves emerge in flatband Heisenberg quantum spin systems. This phenomenon is rather general for a variety of frustrated spin systems in one, two, and three dimensions as well as for Hubbard systems.

I. INTRODUCTION

Ever-lasting oscillations are a fascinating phenomenon that got a new twist with the advent of time crystals [1–4], where a quantum system exhibits oscillatory behaviour of some of its observables. Although a wider notion of time crystals was introduced in [5] (compare in particular Fig. 8) the phenomenon has been narrowed to systems exhibiting many-body localization where a periodic drive results in sub-harmonic response.

The example we want to discuss in the following belongs to the class of non-driven closed Hamiltonian systems, and thus has got some relationship with quantum scars [6–10] as well as Hilbert space fragmentation [11–14]. The appearance of quantum scars, Hilbert space fragmentation, or time crystals signals non-ergodic/non-thermalizing behavior that contradicts our expectation of thermalization that nowadays is the natural expectation for generic quantum systems even when closed, small and under unitary time evolution [15–30]. In order not to interfere with the still evolving notion of time crystals we prefer to qualify the persistent oscillatory dynamics discussed in this article as sufficiently non-trivial (compared to trivial Bloch oscillations or single-spin Larmor precessions [1]). Moreover, as we are going to show, it is related to the observation of solitary waves and transport in quantum spin systems and thus has got connections to quantum magnetism [31, 32].

Magnetic solitons have been detected experimentally in several magnetic systems [35–39] for instance as domain-wall or envelope solitons. From a theoretical point of view magnetic solitons are solutions of non-linear differential equations as for instance the cubic Schrödinger equation [31, 40]. Such non-linear differential equations arise as the result of an approximation of the (ordinary) time-dependent Schrödinger equation, which is linear. For instance, a cubic Schrödinger equation is obtained when quantum spins are replaced by a classical spin density [41].

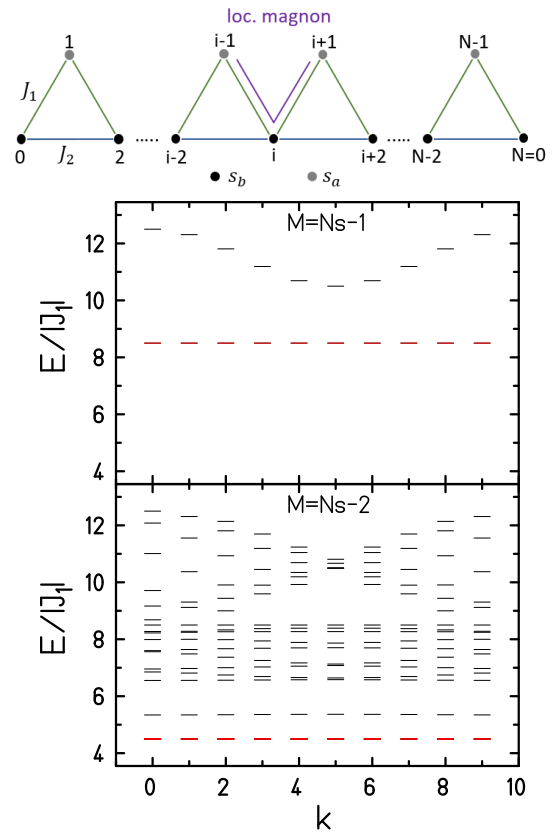


Figure 1. Top: Structure of the delta chain with apical spins s_a and basal spins s_b as well as exchange interactions J_1 and J_2 . The spins are numbered $0, 1, \dots, N-1$. Periodic boundary conditions are applied, i.e. $N \equiv 0$. An independent localized one-magnon state is highlighted that extends over three neighboring sites as indicated [33]. Bottom: Energy eigenvalues for $N = 20$ and $s_a = s_b = \frac{1}{2}$ for one-magnon ($M = Ns-1$) and two-magnon space ($M = Ns-2$). The momentum quantum number k (wave number) runs from 0 to $N/2-1$, compare [34].

As discussed already in Ref. [32], the *linear* time-dependent Schrödinger equation allows for solutions that move along or across some translationally symmetric quantum spin system with frozen shape. Such states

* jeckseler@physik.uni-bielefeld.de

† jschnack@uni-bielefeld.de

shall be called solitary waves. More precisely, we want to call $|\Psi_s\rangle$ a solitary wave if there exists a minimal time $\tau > 0$ for which the time evolution equals (up to a global phase) the shift by one unit cell of the spin system [32]. A state $|\Psi_s\rangle$ that is a superposition of simultaneous eigenstates of energy and momentum $|k, E = \gamma k + E_0\rangle, k = 0, 1, 2, \dots$ with a linear dispersion relation between the energy eigenvalues E and the momentum quantum numbers $k = p/\hbar$ would behave as a solitary wave and move on forever on the respective lattice. With periodic boundary conditions as for instance naturally given in spin rings this would lead to everlasting revolutions around the closed structure.

While in the spectrum of finite-size quantum spin systems true linear dispersion relations between more than two energy levels are typically unlikely, flatband systems give rise to *perfectly* linear dispersion relations even in non-dense spectra when combining appropriate multi-magnon states [33, 42–48].

In order to demonstrate the idea as well as the resulting dynamics we choose the one-dimensional delta chain in the Heisenberg model with spins $s = 1/2$ as a model system which exhibits flat bands in several multimagnon subspaces for a ratio of the two defining exchange interactions of $J_2/J_1 = 1/2$, compare Fig. 1. We find it remarkable that flatband spin systems such as the delta chain as well as all many other systems such as kagome, square-kagome, pyrochlore etc. thus give rise to two rather different phenomena: disorder-free localization with zero group velocity [8, 34] as well as solitary dynamics demonstrated in this paper.

The paper is organized as follows. In Section II we introduce the model, repeat the concepts of independent localized magnons as well as flat bands and explain how initial states are prepared. Section III demonstrates numerical examples of the everlasting revolution and their stability. The article closes with a discussion in Section IV.

II. ESSENTIAL PROPERTIES OF FLATBAND SYSTEMS

The antiferromagnetic delta chain, also termed sawtooth chain, is shown in Fig. 1 (top). It is modelled by the Heisenberg model with periodic boundary conditions

$$\tilde{H} = -2J_1 \sum_{i=0}^{N-1} \tilde{s}_i \cdot \tilde{s}_{i+1} - 2J_2 \sum_{i=0}^{\frac{N}{2}-1} \tilde{s}_{2i} \cdot \tilde{s}_{2i+2}. \quad (1)$$

\tilde{s}_i denotes the spin vector operator at site i , and $J_1 < 0$ as well as $J_2 < 0$ are antiferromagnetic exchange interactions. The unit cell contains two spins which gives rise to momentum quantum numbers $k = 0, 1, \dots, N/2 - 1$. Overall, the eigenstates can be organized according to the present symmetries and labeled with total spin S , total magnetic quantum number M , and momentum quantum number (wave number) k . The Hilbert space decays into

mutually orthogonal subspaces according to these quantum numbers. In general, the sawtooth chain is not integrable.

In one-magnon space two energy bands appear of which one is flat for $J_2/J_1 = 1/2$, see Fig. 1 (center). This property is equivalent to the existence of localized independent one-magnon states (sometimes also termed “compact localized states” [48–50]) of which one is shown in Fig. 1 (top). These states can be constructed systematically, compare [33, 47], as

$$|\text{loc}, i\rangle = \frac{1}{\sqrt{12s_a}} \left(\tilde{s}_{i-1}^- - 2\frac{\sqrt{s_a}}{\sqrt{s_b}} \tilde{s}_i^- + \tilde{s}_{i+1}^- \right) |\Omega\rangle, \\ |\Omega\rangle = |m_0 = s_b, m_1 = s_a, \dots, m_{N-1} = s_a\rangle, \quad (2)$$

where $|\Omega\rangle$ is called magnon vacuum. The localized independent one-magnon states are not only eigenstates of the Hamiltonian in one-magnon space, but also (relative) ground states in this space since they are given by Fourier transforms of the respective ground-state flat band in one-magnon space [33]. Out of localized independent one-magnon states one can construct n -magnon states that are also eigen- and relative groundstates of the Hamiltonian in their respective n -magnon spaces up to the maximum possible number of localized independent magnons [33, 51], compare 2-magnon space in Fig. 1 (bottom). This leads to a strict linear dispersion between magnetic quantum number M and ground state energy of the $(Ns - M)$ -magnon space.

The desired linear dispersion relation between E and k is then obtained by picking appropriate eigenstates $|M, k, \alpha\rangle$ from the respective degenerate ground state manifold. α serves as a label to enumerate the levels within the subspace of degenerate ground states with a certain M and k . To be specific,

$$|\Psi_s\rangle = c_0 |M = Ns, k = 0\rangle + c_1 |M = Ns - 1, k = 1, \alpha_1\rangle + c_2 |M = Ns - 2, k = 2, \alpha_2\rangle \dots, \quad (3)$$

where the first state is the magnon vacuum, the second state a ($k = 1$)-eigenstate from the flat ground state band in one-magnon space, the third a ($k = 2$)-eigenstate from the flat ground state band in two-magnon space, and so on. We consider a superposition of more than two eigenstates as non-trivial because it is unlikely for generic finite-size systems that more than two eigenstates fulfill a linear dispersion relation *exactly*.

In general, with \tilde{U} being the time-evolution operator and \tilde{T} the operator that translates (shifts) by one unit cell, solitary waves $|\Psi_s\rangle$ fulfill

$$\tilde{U}(\tau) |\Psi_s\rangle = e^{-i\phi_0} \tilde{T}^\pm |\Psi_s\rangle \quad (4)$$

for a certain discrete time τ (up to a global phase). Inserting decomposition (3) yields

$$E_\mu \tau / \hbar = \pm \frac{4\pi k_\mu}{N} (+2\pi m_\mu + \phi_0), \quad m_\mu \in \mathbb{Z} \quad (5)$$

mentioned above with some arbitrary constants in parenthesis due to properties of the complex unit circle. This results in a minimal τ of

$$\tau = \frac{\Delta k 4\pi\hbar}{\Delta E N} , \quad (6)$$

where we show \hbar explicitly for convenience [32]. Δk and ΔE are differences according to (5).

To some extent, solitary waves can be shaped depending on the number, kind, and amplitude of its Fourier components, compare (3). In general, more Fourier components with a broader range of momenta yield smaller distributions in space. In addition, even for a fixed k several eigenstates can be picked since the flat band states are often degenerate. However, the construction principle (3) acts as a limiting condition. In addition, as we are going to see, the spacial variance of the expectation value of a local observable depends on the specific observable and in particular on how many different orthogonal subspaces it connects. The operator \tilde{s}_i^x , which we are going to use, connects only eigenstates with $\Delta M = \pm 1$, which then displays only limited parts of the solitary wave (3).

In general, one could say that the solitary wave is probed by the respective employed operators, and the result shows a stroboscopic representation of it. For the same solitary wave such representations can be very different. As an example, the operator \tilde{s}_i^z would basically show the mean magnetic moment due to symmetry, whereas \tilde{s}_i^x uncovers the discussed modulation along the chain. Higher-order operators would shed light on other details of the solitary wave.

III. NUMERICAL EXAMPLES

A. Main result

We looked at a delta chain with $N = 32$ and $s = 1/2$ at the flatband point $J_2/J_1 = 1/2$ where this model is a typical representative of strongly frustrated spin systems hosting flat bands. Figure 2 shows the time evolution of the absolute value of the expectation value of individual operators \tilde{s}_ℓ^x

$$\langle \tilde{s}_\ell^x \rangle = \langle \Psi_s | \tilde{s}_\ell^x | \Psi_s \rangle \quad (7)$$

as a function of time for a superposition of five energy eigenstates with $k = 0, 1, 2, 3, 4$. One recognises two features: (1) every individual spin expectation value oscillates permanently, and (2) this oscillation has got an offset (of size τ) with respect to the neighboring unit cell. In total, the picture shows a wave that travels around the delta-chain with periodic boundary conditions.

The pattern seen for a local observable depends on which components this observable picks out of the superposition. Since the operator \tilde{s}_ℓ^x connects only basis states with $\Delta M = \pm 1$ the construction principle (3) leads to

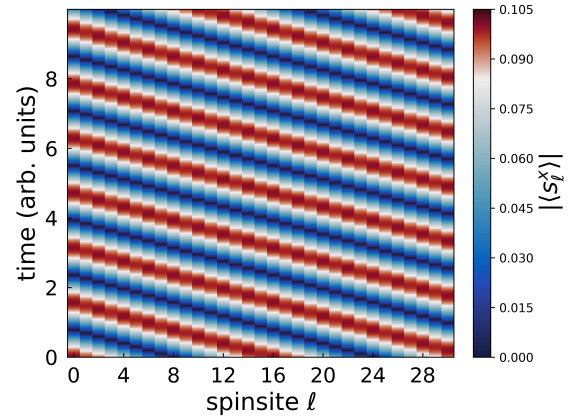


Figure 2. Time evolution of the absolute values of expectation values $|\langle \tilde{s}_\ell^x(t) \rangle|$ in a delta chain with $N = 32$ spins. The initial state is a superposition of five eigenstates according to (3). The characteristic time τ can be deduced from the shift by one unit cell (of two neighboring spins).

terms in the expectation value that contain only terms with $\Delta k = \pm 1$ due to the correlation between M and k in (3). Figure 3 shows the resulting expectation values of $\langle \tilde{s}_\ell^x \rangle$ as well as $|\langle \tilde{s}_\ell^x \rangle|$ for some moment in time. Different operators as well as different construction principles would yield different patterns.

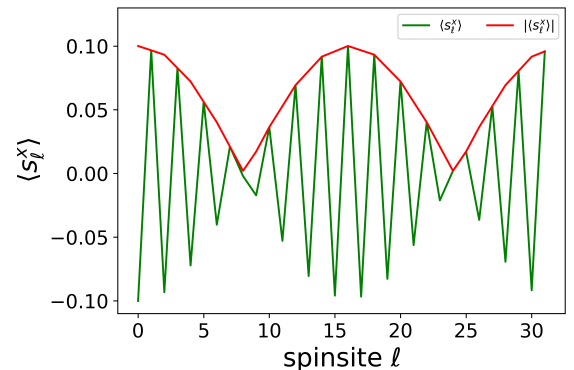


Figure 3. $\langle \tilde{s}_\ell^x \rangle$ and $|\langle \tilde{s}_\ell^x \rangle|$ of an initial solitary wave in a delta chain with $N = 32$. It can be seen that $|\langle \tilde{s}_\ell^x \rangle|$ has two peaks over the whole lattice.

The perpetual motion visible in Fig. 2 can be corroborated by inspection of spin currents along the delta chain. We investigated

$$\tilde{j}^z = -i \sum_\ell \left[\tilde{H}, \tilde{s}_\ell^z \right] , \quad (8)$$

and this current is indeed non-zero for the initial states (3) that we investigate. Depending on the k -values present in the superposition (3) the current runs clockwise or anticlockwise around the sawtooth chain with periodic boundary conditions. The overall dynamics can be pictured as a screw where the screw moves along the

z -direction (current) and the x - and y -components of the local magnetization rotate according to the handedness of the screw which can also be inferred from Fig. 2. In a broader sense this is related to the observation of spin currents in Heisenberg spin systems [52–54], but here it serves to support our claim on the perpetual motion of quantum superpositions given by (3).

B. Stability

The flatband point $J_2/J_1 = 1/2$ defines a fine-tuned Hamiltonian. One could wonder how robust the dynamics is under disturbances. One possible disturbance concerns the initial state (3) that might have additional components not compatible with the construction principle. Figure 4 shows the time evolution of an example where some random Gaussian contributions have been added to (3). Since the differential equation is linear these components develop independently of the perfect state (3). It does appear that the revolving solitary contribution is still clearly visible on top of the Gaussian noise.

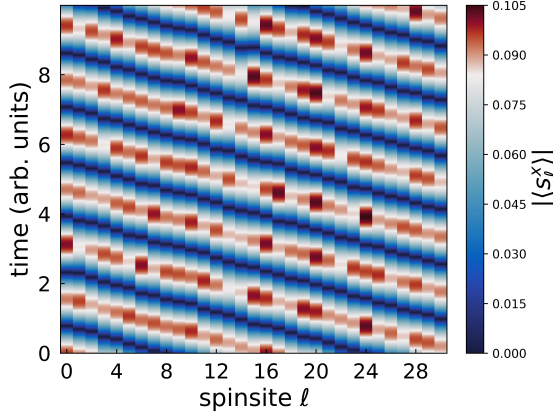


Figure 4. Time evolution of the absolute values of expectation values $|\langle \tilde{s}_\ell^x(t) \rangle|$ in a delta chain with $N=32$ spins. The initial state is a superposition of five eigenstates according to (3) plus a random Gaussian admixture (each complex entry in the representation of a state from the subspace is drawn from a Gaussian distribution with mean 0 and standard deviation of 0.45).

Another disturbance consists in moving away from the flat band point. This situation is covered by Fig. 5, where a slightly dispersive band was chosen that corresponds to $J_2/J_1 = 0.45$. Also here, for a slight disturbance the revolving motion is observable for some time. However, one must clearly say that deviations from the perfect flat band lead to destruction of periodic motion for longer times.

A measure for the stability of the solitary wave is the overlap of the shifted state with the time evolved one (related to the Jozsa fidelity [55] after one revolution around

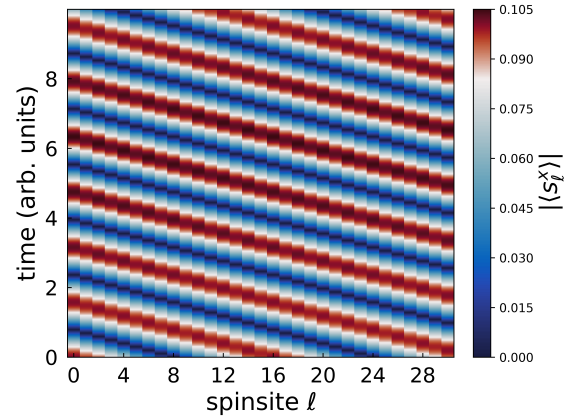


Figure 5. Time evolution of the absolute values of expectation values $|\langle \tilde{s}_\ell^x(t) \rangle|$ in a delta chain with $N=32$ spins and a slightly dispersive band ($J_2/J_1 = 0.45$). The initial state is a superposition of five eigenstates according to (3).

the ring)

$$\eta(t) = \langle \Psi_s | \tilde{U}^{-1} \tilde{U}(t) | \Psi_s \rangle, \tau/2 \leq t < 3\tau/2. \quad (9)$$

We define $\eta(t)$ piece-wise and restart the procedure for the next interval accordingly. For a perfect solitary wave the absolute value of $\eta(n\tau)$, $n \in \mathbb{Z}$, is equal to 1.

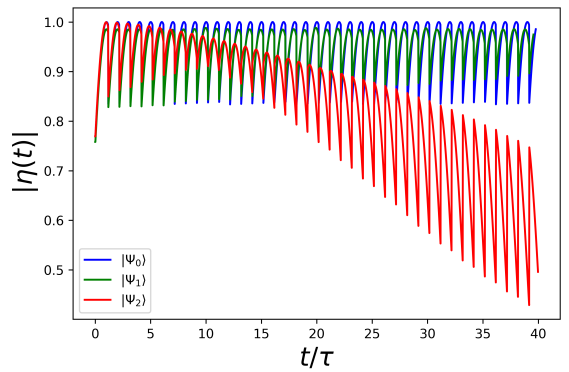


Figure 6. Overlap $\eta(t)$ of the shifted state with the time evolved state for a perfect solitary wave $|\Psi_0\rangle$ (blue), a solitary wave perturbed with a random admixture $|\Psi_1\rangle$ (green) and an approximate solitary wave in a system with a slightly dispersive band $|\Psi_2\rangle$ (red). For the latter case an approximate, effective τ was used as unit of time.

This is seen in Fig. 6 when looking at the blue curve that shows the case of a perfect solitary wave $|\Psi_0\rangle = |\Psi_s\rangle$. If some random component is added to a perfect solitary wave, resulting in $|\Psi_1\rangle$, $|\eta(t)|$ in general will not return to its initial value. However, $|\eta(t)|$ periodically returns to some smaller value since the contribution of the solitary wave develops independently of the remainder for the linear Schrödinger equation. The random component might even equilibrate, i.e., smear out around the ring while the solitary-wave contribution still

runs unperturbed (green curve), see discussion in [34]. If the Hamiltonian is slightly off the flatband scenario, i.e., possesses only dispersive bands, an approximate solitary wave $|\Psi_2\rangle$ slowly loses recurrence, and $|\eta(t)|$ decays while still oscillating (red curve in Fig. 6).

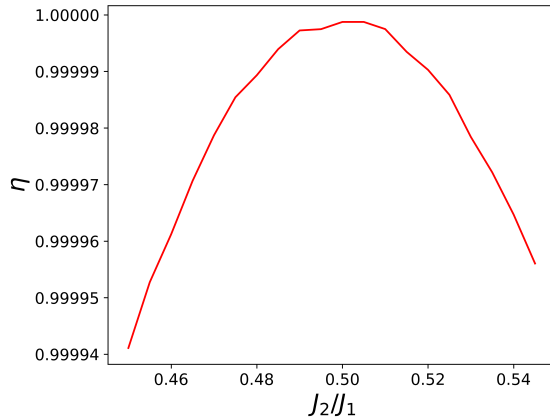


Figure 7. Numerical overlap η of the shifted state with the time evolved state for the next approximate recurrence as function of J_2/J_1 . The initial state is the same as in Fig. 2. For $J_2/J_1 = 1/2$ the recurrence is perfect, the slight deviation from 1.0 is due to the discretization step of the numerical time integration. For $J_2/J_1 \neq 1/2$ η stays astonishingly close to one, but of course drops with detuning away from $J_2/J_1 = 1/2$.

Figure 7 sketches a stability diagram for the initial state used in Fig. 2 for various ratios J_2/J_1 . For $J_2/J_1 = 1/2$ the recurrence is perfect, the slight deviation from 1.0 is due to the discretization step of the numerical time integration that does not hit the exact recurrence time. For $J_2/J_1 \neq 1/2$ η stays astonishingly close to one, but of course drops with detuning away from $J_2/J_1 = 1/2$. This observation means that even in cases where the band is not perfectly flat a perpetual motion can be followed over several cycles.

IV. DISCUSSION AND CONCLUSIONS

In this paper, we demonstrated that certain carefully prepared initial states of flatband systems give rise to permanent oscillations and solitary wave behavior. We would like to remind the reader that a magnetic field is not involved. Quantum spin systems with flat bands such as the discussed delta chain, the kagome lattice, the square-kagome lattice, the pyrochlore lattice and several other frustrated systems thus do not only show very exciting magnetic properties like spin-liquid behavior, magnetization plateaus and jumps, they also provide examples of non-generic, non-ergodic behavior expressed for instance in disorder-free localization with zero group velocity [8, 34] as well as persistent motion of solitary waves. This very general phenomenon also holds for Hubbard models with flat bands [42, 48, 56–65]. In a forthcoming publication the phenomenon will be discussed for the technically more demanding two-dimensional kagome lattice antiferromagnet [66] based on a recent thesis [67].

Of course, the peculiar dynamics is related to fine-tuned Hamiltonians and sometimes also fine-tuned initial states. Away from the flatband scenario, strictly permanent oscillations will not occur, however, depending on the strength of the dispersion they might be very long-lived. For further thoughts on the decay of long-lived oscillations see [68].

Experimentally, the needed initial states could be excited by means of electron paramagnetic resonance (EPR) at low temperature close to the saturation field. The strong correlation between magnetic quantum number and momentum quantum number works in favor of a balanced population of the needed components.

New developments point at flat bands accessible at small fields. These flat band systems are characterized by ferromagnetic as well as antiferromagnetic interactions [69–72] or special XXZ interactions [73–75].

ACKNOWLEDGMENT

This work was supported by the Deutsche Forschungsgemeinschaft DFG (355031190 (FOR 2692); 397300368 (SCHN 615/25-2)). We acknowledge support for the publication costs by the Open Access Publication Fund of Bielefeld University and the DFG.

- [1] F. Wilczek, Quantum time crystals, *Phys. Rev. Lett.* **109**, 160401 (2012).
- [2] M. Medenjak, B. Buča, and D. Jaksch, Isolated Heisenberg magnet as a quantum time crystal, *Phys. Rev. B* **102**, 041117(R) (2020).
- [3] P. Hannaford and K. Sacha, A decade of time crystals: Quo vadis?, *Europhys. Lett.* **139**, 10001 (2022).
- [4] P. Reimann, P. Vorndamme, and J. Schnack, Nonequilibrium, synchronization, and time crystals in isotropic Heisenberg models, *Phys. Rev. Res.* **5**, 043040 (2023).
- [5] V. Khemani, R. Moessner, and S. L. Sondhi, A brief history of time crystals, *arXiv:1910.10745* (2019).
- [6] C. J. Turner, A. A. Michailidis, D. A. Abanin, M. Serbyn, and Z. Papić, Weak ergodicity breaking from quantum many-body scars, *Nat. Phys.* **14**, 745 (2018).
- [7] W. W. Ho, S. Choi, H. Pichler, and M. D. Lukin, Periodic orbits, entanglement, and quantum many-body scars in constrained models: Matrix product state ap-

proach, *Phys. Rev. Lett.* **122**, 040603 (2019).

[8] P. A. McClarty, M. Haque, A. Sen, and J. Richter, Disorder-free localization and many-body quantum scars from magnetic frustration, *Phys. Rev. B* **102**, 224303 (2020).

[9] Y. Kuno, T. Mizoguchi, and Y. Hatsugai, Flat band quantum scar, *Phys. Rev. B* **102**, 241115(R) (2020).

[10] S. Pilatowsky-Cameo, D. Villaseñor, M. A. Bastarrachea-Magnani, S. Lerma-Hernández, L. F. Santos, and J. G. Hirsch, Ubiquitous quantum scarring does not prevent ergodicity, *Nat. Commun.* **12**, 852 (2021).

[11] V. Khemani, M. Hermele, and R. Nandkishore, Localization from Hilbert space shattering: From theory to physical realizations, *Phys. Rev. B* **101**, 174204 (2020).

[12] B. Buća, Out-of-time-ordered crystals and fragmentation, *Phys. Rev. Lett.* **128**, 100601 (2022).

[13] S. Moudgalya, B. A. Bernevig, and N. Regnault, Quantum many-body scars and Hilbert space fragmentation: a review of exact results, *Rep. Prog. Phys.* **85**, 086501 (2022).

[14] M. Will, R. Moessner, and F. Pollmann, Realization of Hilbert space fragmentation and fracton dynamics in two dimensions, *Phys. Rev. Lett.* **133**, 196301 (2024).

[15] J. M. Deutsch, Quantum statistical mechanics in a closed system, *Phys. Rev. A* **43**, 2046 (1991).

[16] M. Srednicki, Chaos and quantum thermalization, *Phys. Rev. E* **50**, 888 (1994).

[17] J. Schnack and H. Feldmeier, Statistical properties of fermionic molecular dynamics, *Nucl. Phys. A* **601**, 181 (1996).

[18] J. Schnack and H. Feldmeier, The nuclear liquid–gas phase transition within fermionic molecular dynamics, *Phys. Lett. B* **409**, 6 (1997).

[19] H. Tasaki, From quantum dynamics to the canonical distribution: General picture and a rigorous example, *Phys. Rev. Lett.* **80**, 1373 (1998).

[20] M. Rigol, V. Dunjko, and M. Olshanii, Thermalization and its mechanism for generic isolated quantum systems, *Nature* **452**, 854 (2008).

[21] P. Reimann, Foundation of statistical mechanics under experimentally realistic conditions, *Phys. Rev. Lett.* **101**, 190403 (2008).

[22] A. Polkovnikov, K. Sengupta, A. Silva, and M. Vengalattore, Colloquium, *Rev. Mod. Phys.* **83**, 863 (2011).

[23] P. Reimann and M. Kastner, Equilibration of isolated macroscopic quantum systems, *N. J. Phys.* **14**, 043020 (2012).

[24] A. J. Short and T. C. Farrelly, Quantum equilibration in finite time, *N. J. Phys.* **14**, 013063 (2012).

[25] R. Steinigeweg, A. Khodja, H. Niemeyer, C. Gogolin, and J. Gemmer, Pushing the limits of the eigenstate thermalization hypothesis towards mesoscopic quantum systems, *Phys. Rev. Lett.* **112**, 130403 (2014).

[26] C. Gogolin and J. Eisert, Equilibration, thermalisation, and the emergence of statistical mechanics in closed quantum systems, *Rep. Prog. Phys.* **79**, 056001 (2016).

[27] L. D’Alessio, Y. Kafri, A. Polkovnikov, and M. Rigol, From quantum chaos and eigenstate thermalization to statistical mechanics and thermodynamics, *Adv. Phys.* **65**, 239 (2016).

[28] F. Borgonovi, F. M. Izrailev, L. F. Santos, and V. G. Zelevinsky, Quantum chaos and thermalization in isolated systems of interacting particles, *Phys. Rep.* **626**, 1 (2016).

[29] M. Schiulaz, M. Tavora, and L. F. Santos, From few- to many-body quantum systems, *Quantum Sci. Technol.* **3**, 044006 (2018).

[30] P. Reimann and J. Gemmer, Why are macroscopic experiments reproducible? Imitating the behavior of an ensemble by single pure states, *Physica A* **552**, 121840 (2020).

[31] H. J. Mikeska and M. Steiner, Solitary excitations in one-dimensional magnets, *Adv. Phys.* **40**, 191 (1991).

[32] J. Schnack and P. Shchelokovskyy, Solitary waves on finite-size antiferromagnetic quantum Heisenberg spin rings, *J. Magn. Magn. Mater.* **306**, 79 (2006).

[33] J. Schnack, H.-J. Schmidt, J. Richter, and J. Schulenburg, Independent magnon states on magnetic polytopes, *Eur. Phys. J. B* **24**, 475 (2001).

[34] F. Johannesmann, J. Eckeler, H. Schlüter, and J. Schnack, Nonergodic one-magnon magnetization dynamics of the antiferromagnetic delta chain, *Phys. Rev. B* **108**, 064304 (2023).

[35] M. Köppen, M. Lang, R. Helfrich, F. Steglich, P. Thalmeier, B. Schmidt, B. Wand, D. Pankert, H. Benner, H. Aoki, and A. Ochiai, Solitary magnetic excitations in the low-carrier density, one-dimensional $s = \frac{1}{2}$ antiferromagnet Yb_4As_3 , *Phys. Rev. Lett.* **82**, 4548 (1999).

[36] F. H. L. Eßler, Sine-Gordon low-energy effective theory for copper benzoate, *Phys. Rev. B* **59**, 14376 (1999).

[37] T. Asano, H. Nojiri, Y. Inagaki, J. P. Boucher, T. Sakon, Y. Ajiro, and M. Motokawa, ESR investigation on the breather mode and the spinon-breather dynamical crossover in Cu benzoate, *Phys. Rev. Lett.* **84**, 5880 (2000).

[38] M. Lang, M. Köppen, P. Gegenwart, T. Cichorek, P. Thalmeier, F. Steglich, and A. Ochiai, Evidence for magnons and solitons in the one-dimensional $s = 1/2$ antiferromagnet Yb_4As_3 , *Physica B* **281&282**, 458 (2000).

[39] H. Nojiri, T. Asano, Y. Ajiro, H. Kageyama, Y. Ueda, and M. Motokawa, High-field ESR on quantum spin systems, *Physica B* **294&295**, 14 (2001).

[40] H. J. Mikeska, Quantum solitons and the Haldane phase in antiferromagnetic spin chains, *Chaos Solitons Fractals* **5**, 2585 (1995).

[41] D. C. Mattis, *The theory of magnetism I*, 2nd ed., Solid-State Science, Vol. 17 (Springer, Berlin, Heidelberg, New York, 1988).

[42] A. Mielke and H. Tasaki, Ferromagnetism in the Hubbard-model – examples from models with degenerate single-electron ground-states, *Commun. Math. Phys.* **158**, 341 (1993).

[43] J. Schulenburg, A. Honecker, J. Schnack, J. Richter, and H.-J. Schmidt, Macroscopic magnetization jumps due to independent magnons in frustrated quantum spin lattices, *Phys. Rev. Lett.* **88**, 167207 (2002).

[44] Blundell, S. A. and Núñez-Regueiro, M. D., Quantum topological excitations: from the sawtooth lattice to the Heisenberg chain, *Eur. Phys. J. B* **31**, 453 (2003).

[45] M. E. Zhitomirsky and H. Tsunetsugu, Exact low-temperature behavior of a kagomé antiferromagnet at high fields, *Phys. Rev. B* **70**, 100403(R) (2004).

[46] O. Derzhko, J. Richter, A. Honecker, M. Maksymenko, and R. Moessner, Low-temperature properties of the Hubbard model on highly frustrated one-dimensional lattices, *Phys. Rev. B* **81**, 014421 (2010).

[47] O. Derzhko, J. Richter, and M. Maksymenko, Strongly correlated flat-band systems: The route from Heisenberg spins to Hubbard electrons, *Int. J. Mod. Phys. B* **29**, 1530007 (2015).

[48] D. Leykam, A. Andreeanov, and S. Flach, Artificial flat band systems: from lattice models to experiments, *Advances in Physics: X* **3**, 1473052 (2018).

[49] W. Maimaiti, A. Andreeanov, H. C. Park, O. Gendelman, and S. Flach, Compact localized states and flat-band generators in one dimension, *Phys. Rev. B* **95**, 115135 (2017).

[50] Y. Chen, J. Huang, K. Jiang, and J. Hu, Decoding flat bands from compact localized states, *Science Bulletin* **68**, 3165 (2023).

[51] H.-J. Schmidt, J. Richter, and R. Moessner, Linear independence of localized magnon states, *J. Phys. A: Math. Gen.* **39**, 10673 (2006).

[52] X. Zotos and P. Prelovšek, Transport in one dimensional quantum systems, in *Strong interactions in low dimensions*, edited by D. Baeriswyl and L. Degiorgi (Springer Netherlands, Dordrecht, 2004) pp. 347–382.

[53] F. Heidrich-Meisner, A. Honecker, and W. Brenig, Transport in quasi one-dimensional spin-1/2 systems, *Eur. Phys. J. Spec. Top.* **151**, 135 (2007).

[54] B. Bertini, F. Heidrich-Meisner, C. Karrasch, T. Prosen, R. Steinigeweg, and M. Žnidarič, Finite-temperature transport in one-dimensional quantum lattice models, *Rev. Mod. Phys.* **93**, 025003 (2021).

[55] R. Jozsa, Fidelity for mixed quantum states, *J. Mod. Opt.* **41**, 2315 (1994).

[56] A. Mielke, Ferromagnetism in the Hubbard model on line graphs and further considerations, *J. Phys. A: Math. Gen.* **24**, 3311 (1991).

[57] A. Mielke, Ferromagnetic ground states for the Hubbard model on line graphs, *J. Phys. A: Math. Gen.* **24**, L73 (1991).

[58] A. Mielke, Exact ground-states for the Hubbard-model on the kagome lattice, *J. Phys. A-Math. Gen.* **25**, 4335 (1992).

[59] H. Tasaki, Ferromagnetism in the Hubbard models with degenerate single-electron ground states, *Phys. Rev. Lett.* **69**, 1608 (1992).

[60] H. Tasaki, From Nagaoka’s ferromagnetism to flat-band ferromagnetism and beyond – an introduction to ferromagnetism in the Hubbard model, *Prog. Theor. Phys.* **99**, 489 (1998).

[61] E. J. Bergholtz and Z. Liu, Topological flat band models and fractional Chern insulators, *Int. J. Mod. Phys. B* **27**, 1330017 (2013).

[62] O. Derzhko, J. Richter, and M. Maksymenko, Strongly correlated flat-band systems: The route from Heisenberg spins to Hubbard electrons, *Int. J. Mod. Phys. B* **29**, 1530007 (2015).

[63] M. Maksymenko, R. Moessner, and K. Shtengel, Persistence of the flat band in a kagome magnet with dipolar interactions, *Phys. Rev. B* **96**, 134411 (2017).

[64] S. Tilleke, M. Daumann, and T. Dahm, Nearest neighbour particle-particle interaction in fermionic quasi one-dimensional flat band lattices, *Z. Naturforsch. A* **75**, 393 (2020).

[65] M. Daumann and T. Dahm, Anomalous diffusion, prethermalization, and particle binding in an interacting flat band system, *N. J. Phys.* **26**, 063001 (2024).

[66] H. Schlüter, J. Eckseler, and J. Schnack, Non-ergodic one-magnon magnetization dynamics of the kagome lattice antiferromagnet, manuscript in preparation.

[67] H. Schlüter, *Zu dynamischen und thermodynamischen Eigenschaften frustrierter Spinsysteme mit flachen Energiebändern*, Ph.D. thesis, Bielefeld University, Faculty of Physics (2024).

[68] J. H. Robertson, R. Senese, and F. H. L. Essler, Decay of long-lived oscillations after quantum quenches in gapped interacting quantum systems, *Phys. Rev. A* **109**, 032208 (2024).

[69] V. Y. Krivnov, D. V. Dmitriev, S. Nishimoto, S.-L. Drechsler, and J. Richter, Delta chain with ferromagnetic and antiferromagnetic interactions at the critical point, *Phys. Rev. B* **90**, 014441 (2014).

[70] D. V. Dmitriev, V. Y. Krivnov, J. Richter, and J. Schnack, Thermodynamics of a delta chain with ferromagnetic and antiferromagnetic interactions, *Phys. Rev. B* **99**, 094410 (2019).

[71] O. Derzhko, J. Schnack, D. V. Dmitriev, V. Y. Krivnov, and J. Richter, Flat-band physics in the spin-1/2 sawtooth chain, *Eur. Phys. J. B* **93**, 161 (2020).

[72] D. V. Dmitriev and V. Y. Krivnov, Magnetic properties of delta- and kagome-like chains with competing interactions, *J. Phys.: Condens. Matter* **35**, 445802 (2023).

[73] H. J. Changlani, S. Pujari, C.-M. Chung, and B. K. Clark, Resonating quantum three-coloring wave functions for the kagome quantum antiferromagnet, *Phys. Rev. B* **99**, 104433 (2019).

[74] K. Lee, R. Melendrez, A. Pal, and H. J. Changlani, Exact three-colored quantum scars from geometric frustration, *Phys. Rev. B* **101**, 241111 (2020).

[75] S. Pal, P. Sharma, H. J. Changlani, and S. Pujari, Colorful points in the XY regime of XXZ quantum magnets, *Phys. Rev. B* **103**, 144414 (2021).